HHS Public Access

Author manuscript

Environ Toxicol Chem. Author manuscript; available in PMC 2018 April 12.

Published in final edited form as:

Environ Toxicol Chem. 2011 December ; 30(12): 2748–2755. doi:10.1002/etc.701.

SUPPRESSION OF HUMORAL IMMUNE RESPONSES BY 2,3,7,8-TETRACHLORODIBENZO-*p*-DIOXIN INTERCALATED IN SMECTITE CLAY

Stephen A. Boyd[*,†], **Cliff T. Johnston**[‡], **Thomas J. Pinnavaia**[§], **Norbert E. Kaminski**[‖,#], **Brian J. Teppen**[†], **Hui Li**[†], **Bushra Khan**[‡], **Robert B. Crawford**[‖,#], **Natalia Kovalova**[‖,#], **Seong-Su Kim**[§], **Hua Shao**[§], **Cheng Gu**[†], and **Barbara L.F. Kaplan**[‖,#]

[†]Department of Crop and Soil Sciences, Michigan State University, East Lansing, Michigan, USA

[‡]Crop, Soil and Environmental Sciences, Purdue University, West Lafayette, Indiana, USA

[§]Department of Chemistry, Michigan State University, East Lansing, Michigan, USA

[‖]Center for Integrative Toxicology, Michigan State University, East Lansing, Michigan, USA

[#]Department of Pharmacology and Toxicology, Michigan State University, East Lansing, Michigan, USA

Abstract

2,3,7,8-Tetrachlorodibenzo-*p*-dioxin (TCDD) is a highly toxic environmental contaminant found in soils and sediments. Because of its exceptionally low water solubility, this compound exists predominantly in the sorbed state in natural environments. Clay minerals, especially expandable smectite clays, are one of the major component geosorbents in soils and sediments that can function as an effective adsorbent for environmental dioxins, including TCDD. In this study, TCDD was intercalated in the smectite clay saponite by an incipient wetness method. The primary goal of this study was to intercalate TCDD in natural K-saponite clay and evaluate its immunotoxic effects in vivo. The relative bioavailability of TCDD was evaluated by comparing the metabolic activity of TCDD administered in the adsorbed state as an intercalate in saponite and freely dissolved in corn oil. This comparison revealed nearly identical TCDD-induced suppression of humoral immunity, a well-established and sensitive sequela, in a mammalian (mouse) model. This result suggests that TCDD adsorbed by clays is likely to be available for biouptake and biodistribution in mammals, consistent with previous observations of TCDD in livestock exposed to dioxin-contaminated ball clays that were used as feed additives. Adsorption of TCDD by clay minerals does not appear to mitigate risk associated with TCDD exposure substantially.

Keywords

Sorption; Bioavailability; Dioxin; Clay mineral; Soil toxicology

[*]To whom correspondence may be addressed (boyds@msu.edu).

INTRODUCTION

The potential for aluminosilicate clays to function as effective adsorbents for polychlorinated dibenzo-*p*-dioxins (PCDDs) has been demonstrated in recent studies that have shown that certain smectite clays were highly effective for the removal of dibenzo-*p*-dioxin from water [1,2]. In addition, clay-PCDD associations have been reported in diverse geologic settings that include North America [3–6], Germany [7], and Australia [8,9].

Mechanistic studies on the adsorption of dioxins by clays have revealed that smectite clays with low (negative) layer charge resulting from tetrahedral substitution that is neutralized by relatively weakly hydrated cations (K^+, NH_4^+, Cs^+) manifest optimal adsorptive affinities for a variety of neutral organic contaminants (NOCs) [10–12], including dibenzo-*p*-dioxin [1]. These structural parameters maximize adsorption domains parallel to the siloxane clay surfaces while optimizing adsorption domains perpendicular to the clay surface [10,11]. A homoionic Cs-saturated saponite embodies these characteristics and demonstrates high adsorption affinity and capacity for dibenzo-*p*-dioxin [1,2]. In such a clay, dibenzo-*p*-dioxin resides primarily in the clay interlayers, i.e., is intercalated, and may orient parallel to the plane of the clay layers at lower loadings or in a nonparallel (tilted) arrangement at higher (~0.8% wt/wt) loadings [1,2]. These dibenzo-*p*-dioxin intercalates form favorably because they maximize interactions of the dibenzo-*p*-dioxin ring structure with the siloxane sheets of opposing clay layers, interactions of Cs^+ with the dioxin ring oxygens, and solute dehydration in the subaqueous environment of the clay galley regions [1,2,10,13]. Homoionic K-smectites typically display similar, but reduced, adsorptive characteristics for NOCs [10,12,14]. Other sorbent phases for PCDDs in soils and sediments include amorphous organic matter and carbonaceous geosorbents such as chars [15–17].

In the context of exposure to soil- and sediment-borne contaminants, bioavailability processes is a useful term defined as “the individual physical, chemical, and biological interactions that determine the exposure of organisms to chemicals associated with soils and sediments” [18]. It includes contaminant binding to and release from soils and sediments, movement of the contaminant (in the free or bound form) to the membrane of the organism, movement from the external environment through a physiological barrier of a living system (uptake across a membrane), and exertion of a toxicological effect. The term *bioavailability*, as it is used herein, encompasses the entire set of bioavailability processes. Examination of the existing literature by Kimbrough et al. ([19], and references therein) reveals that the human uptake of soil-borne polychlorinated dibenzo-*p*-dioxins and furans (PCDD/Fs) is certainly poorly understood. We contend that much of this variability and confusion stems from the inherent complexity and heterogeneity of soils, often confounded by the presence of anthropogenic sorbent phases such as residual oils [20] and graphitic carbon [21], which have been ignored or poorly understood in previous studies of bioavailability. Other investigators have correctly pointed out the importance of site-specific factors in studies designed to determine oral bioavailability of soil-borne PCDD/Fs [19,21–23], but there is a paucity of data regarding the identity, importance, and specific role of soil-related factors that may act as determinants of bioavailability. Certainly, specific examples indicate that soil-borne PCDD/Fs are at least partially bioavailable. One example comes from a recent

study of PCDD/F body burdens of residents presently living on contaminated soils of the Saginaw–Titta-bawasee floodplain (Midland, MI, USA). The person with the highest PCDD blood level (211 ppt) was a potter known to use PCDD-contaminated ball clays for ceramics that were fired in an unvented in-home kiln [24]. Similarly, PCDD-contaminated ball clays, added to animal feed as an anticaking agent, have resulted in widespread contamination of chickens, farm-raised catfish, and baby food [25–27]. While PCDD/Fs in ball clays are clearly bioavailable to humans and animals to some extent, as they assuredly are in soils, it is impossible to reconcile the measured values of bioavailability, which range from <1 to >50%, without understanding the underlying mechanistic basis of bioavailability.

We contend that understanding the differential bioavailability or human uptake of soil- or sediment-borne NOCs in general, and PCDDs specifically, requires knowledge of the individual role of the major geosorbent types, namely, amorphous organic matter, carbonaceous materials (e.g., chars), and clay minerals, especially smectites. This view was also articulated by Budinsky et al. [22] in a recent study on the bioavailability of PCDD/Fs in soils. To confront the inherent complexity of soil as it relates to human uptake of or exposure to PCDD/Fs present in soils, we report here the toxicity of 2,3,7,8-tetrachlorodibenzo-*p*-dioxin (TCDD) associated with smectite clay, which has previously been shown to function as an effective adsorbent for dioxin [1]. Specifically, the primary goal of this study was to intercalate TCDD into natural K-saponite clay and evaluate its immunotoxic effects in vivo. The activity of TCDD administered in the adsorbed state as an intercalate in saponite, and freely dissolved in corn oil, was compared by measuring suppression of humoral immunity, a well-established and sensitive sequela, in a mammalian (mouse) model. Intercalation of TCDD in the saponite clay interlayer regions was evaluated using structural, spectroscopic, and thermal methods.

MATERIALS AND METHODS

Clay preparation of natural K-saponite

A naturally occurring reference smectite (SapCa-2), obtained from the Source Clays Repository of the Clay Minerals Society at Purdue University, was used in the present study. The major physicochemical characteristics of this clay have been reported by Liu et al. [1]. The <2-μm clay fraction was collected by wet sedimentation, suspended in 0.1 M KCl for 24 h, then centrifuged and resuspended repeatedly to saturate the exchangeable cation sites. Excess salts were removed by rinsing with deionized water. The clay suspension was then quick frozen and freeze dried.

Saponite synthesis

Synthetic saponite was prepared at 90°C according to previously described methods [28,29] using water glass solution (27 wt% silica, 14 wt% NaOH), $Al(NO_3)_3 \cdot 9H_2O$, $Mg(NO_3)_2 \cdot 6H_2O$, and NaOH as reagents. The Si:Al:Mg:NaOH molar ratio of the reaction mixture was 3.6:0.4:3.0:5 per 400 moles water. The stirred reaction mixture was heated for 24 h at 90°C in a three-neck, round-bottom flask, and the resulting product was centrifuged, triple washed with deionized water, and dried at 80°C under N_2 flow before use. The synthetic saponite was prepared to provide a clay with a composition essentially identical to that of natural

saponite (SapCa-2) but a different physical arrangement of clay layers in the aggregates that they form (see below).

Synthetic saponite characterization

X-ray diffraction (XRD) patterns of the synthetic saponite were obtained on a Rigaku rotaflex 200B diffractometer equipped with Cu Kα X-ray radiation and a curved crystal graphite monochromator, operating at 45 kV and 100 mA. The N_2 adsorption–desorption isotherms were recorded at −196°C on a Micromeritics TriStar 3000 sorptometer. Prior to analysis, samples were out-gassed at 150°C and 10^{-6} Torr for a minimum of 12 h. Brunauer–Emmett–Teller (BET) surface areas were calculated from the linear part of the BET plot, and Barrett-Joyner-Halenda pore sizes were obtained from adsorption isotherms.

Transmission electron microscopy images were obtained on a JEOL 2200FS field emission microscope with a ZrO/W Schottky electron gun and an accelerating voltage of 200 kV. The powdered samples were sonified in ethanol and dripped onto 300 mesh copper grids. The ^{29}Si and ^{27}Al magic angle-spinning nuclear magnetic resonance (MAS NMR) spectra were obtained at 79 MHz on a Varian VXR-400S solid-state NMR spectrometer equipped with a magic angle-spinning probe. Sample was spun at 4 kHz for each measurement. The pulse delay for ^{29}Si MAS NMR was 400 s, and chemical shifts were referenced to talc. The pulse delay for ^{27}Al MAS NMR was 0.50 s, and a 0.10 M aqueous $Al(NO_3)_3$ solution was used as the chemical shift reference.

Intercalation of TCDD into natural K-saponite

The TCDD was intercalated into 290 mg natural K-saponite by adding 145 μl of a dimethylsulfoxide (DMSO) solution containing 100 ppm TCDD in a 30-ml Corex centrifuge tube to achieve a final concentration of 50 mg TCDD/kg clay. The proportions of clay to TCDD to DMSO were established in preliminary studies as the minimum amount of DMSO that resulted in the complete expansion of the K-saponite clay to a d-spacing of 1.96 nm. As a control, the same amount of DMSO was added to 290 mg K-saponite without TCDD. To facilitate the redistribution of DMSO–TCDD into the clay interlayers, the samples were sealed and heated at 60°C. Thermogravimetric analysis (TGA), XRD, and Fourier transform infrared (FTIR) spectra of the resulting clay–DMSO–TCDD and clay–DMSO complexes were obtained. An isothermal heat treatment of 200°C for 50 min under a flow of N_2 was used to remove excess DMSO. X-ray diffraction TGA and FTIR spectra of clay–DMSO–TCDD and clay–DMSO complexes were obtained after the isothermal 200°C treatment.

Immobilization of TCDD on synthetic saponite

The TCDD was immobilized on the synthetic saponite by the incipient wetness method. In this procedure, an aliquot of TCDD solution equal to the pore volume of the clay was dropped onto to the surface of the dry clay powder in a glass vial with the use of a hypodermic syringe. To make 13.5 ml of an aqueous gavage suspension, an aliquot containing 0 to 35.5 μl of TCDD dissolved in DMSO (100 ppm), and the remaining volume of DMSO of 88.6 μl minus the volume of the TCDD–DMSO solution, was added to 86 mg synthetic saponite with a pore volume of 88.6 μl. The vial was sealed with an aluminum-lined screw cap, and the mixture was vigorously agitated on a vortex mixer until the liquid

was uniformly dispersed in the powder and the powder was returned to a dry and free-flowing state. The resulting mixture was then equilibrated overnight at 60°C to ensure uniform distribution of the TCDD solution within the pores of the synthetic saponite. After each impregnation, the DMSO solvent was removed from the synthetic saponite in a vacuum oven at 60°C overnight in order to obtain a uniform distribution of TCDD molecules on the basal surfaces of the clay nanolayers. The procedure was repeated for TCDD loadings requiring sequential impregnations to achieve the desired loading. The TCDD-impregnated synthetic saponite was then used to prepare aqueous suspensions for the mouse dosing experiments by adding 13.5 ml H_2O.

Natural K-saponite intercalated with TCDD

Fourier transform infrared spectra of the natural K-saponite–TCDD complex was obtained by using diffuse reflectance (Easy Diff Pike Technologies) on a PerkinElmer GX2000 FTIR spectrometer equipped with a mercury–cadmium–telluride (MCT) detector, a KBr beam splitter, and an MCT detector with a resolution of 4.0 cm^{-1}. A total of 64 scans were collected for each spectrum. Samples for diffuse reflectance analysis were diluted in spectral-grade KBr (Pike Technologies) at a solids concentration of 10% (w/w). Micro-Raman and micro-FTIR spectra of TCDD were collected from a deposit using the drop coating deposition (Raman) method as described by Zhang et al. [30]. An aliquot of 25 μl of a solution containing 10 mg/L TCDD dissolved in toluene (ChemService) was placed on a SpectRIM slide (Tienta Science) and allowed to evaporate, leaving the TCDD crystals. The crystals were very small, thin, and needle-like, and were approximately 15 to 30 μm in length by 2 to 3 μm in width. The FTIRspectra were obtained using a Thermo Scientific Nicolet 6700 FT-IR spectrometer coupled to a Nicolet Continuum FTIR microscope. A rectangular aperture of 50 × 10 μm was used. Background FTIR spectra were obtained from a clean portion of the SpectRIM slide using the same aperture by coaddition of 128 scans using an optical resolution of 2.0 cm^{-1}. The spectrometer/microscope was equipped with an MCT/A detector and a KBr beam splitter. The FTIR spectra were obtained using OMNIC 8 software. Raman spectra of this same deposit of TCDD crystals on the SpectRIM slide were obtained on an Acton Research Corporation SpectroPro500 spectrograph optically coupled to an Olympus BX60 microscope. A ×50 optical objective was used to focus the laser and simultaneously collect Raman scattered light from the TCDD crystals. A Spectra-Physics model 127 HeNe laser (632.8 nm) with an output of 35 mW was used. Raman-scattered radiation was collected in a 180° back-scattering configuration. The entrance slits to the spectrograph were set to 10 μm. The spectrograph used a holographic super notch filter to eliminate Rayleigh scattering. The detector was a Princeton Instruments liquid-N_2-cooled charge-coupled device detector. The spectrograph was calibrated daily using an Ne–Ar calibration lamp based on known spectral lines. X-ray diffraction patterns of the natural K-saponite–DMSO–TCDD and Ksaponite– DMSO complexes were collected using a PANalytical model X'Pert PRO diffractometer and Co Kα radiation. Approximately 150 mg of the clay K-saponite–DMSO–dioxin complexes was mounted on a powder mount. The diffraction patterns were collected from 2 to 80° 2θ, counting for 1 s every 0.02° 2θ step. A 1° exit Soller slit was used. Data were analyzed in X'Pert HighScore Plus software version 2.2 (PANalytical).

For TGA, the K-saponite–DMSO–TCDD and the K-saponite–DMSO samples were weighed in 70-µl ceramic crucibles. The crucibles were placed in the thermogravimetric analyzer (model TGA/SDTA851e; Mettler Toledo) and heated at a rate of 20°C/min under a flow of N_2 until a temperature of 200°C was obtained and held at this temperature for a total run time of 50 min (9 min of heating to 200°C and 41 min of hold time at 200°C). In addition, full mass loss curves were obtained by heating the sample from 25 to 1,000°C at a rate of 20°C/min under a flow of N_2. The data were analyzed in STARe software version 9.0X (Mettler Toledo).

Animals

Pathogen-free female B6C3F1 mice, five to eight weeks of age, were purchased from Charles River Breeding Laboratories. On arrival, mice were randomized, transferred to plastic cages containing sawdust bedding (five animals per cage), and acclimated for at least one week. Mice were provided food (Purina Certified Laboratory Chow) and water ad libitum and were not used for experimentation until their body weight was 17 to 20 g. Animal holding rooms were kept at 21 to 24°C and 40 to 60% relative humidity, with a 12-h light:dark cycle. All procedures involving mice were in accordance with the Michigan State University Institutional Animal Care and Use Committee.

In vivo antibody-forming cell response

Mice (five per treatment group) were administered corn oil vehicle, TCDD, synthetic or natural clay alone, DMSO-adsorbed synthetic or natural clay, or TCDD-adsorbed synthetic or natural clay by oral gavage once per day for 4 consecutive days. The synthetic or natural clay or TCDD-adsorbed synthetic or natural clay was delivered in 200 µl water. On day 3, mice were sensitized with 5×10^8 sheep red blood cells (sRBC) per mouse by intraperitoneally injection to allow for TCDD exposure surrounding antigen sensitization. Four days after sRBC sensitization, mice were sacrificed, and total body and spleen weights were recorded. Enumeration of antibody-forming cells (AFCs) was performed using the Jerne plaque assay [31]. Briefly, 100-µl aliquots of the recovered splenocytes were combined with 0.5% melted agar (Difco/BD), guinea pig complement (Gibco/Invitrogen), and sRBC. The mixture was vortex mixed, poured onto a Petri dish, overlaid with a 24- × 50-mm glass coverslip, and allowed to solidify. The mixture was incubated for at least 3 h at 37°C, after which AFCs were enumerated using a Bellco plaque viewer at ×6.5 magnification (Bellco Glass). Cells were enumerated with a Z1 Coulter particle counter (Beckman Coulter).

Real-time polymerase chain reaction

Livers from the treated mice were placed in TRI reagent (Sigma) and stored at −70°C. On the day of RNA extraction, livers were homogenized. After phase separation with bromochlorophenol, RNA was precipitated from the aqueous phase with isopropanol. The remainder of the extraction, purification, and DNase treatment was performed using the Promega SV total RNA isolation system. Total RNA was reverse transcribed using random primers with the high capacity cDNA reverse transcription kit (Applied Biosystems). cDNA was amplified with a Taqman primer/probe set for mouse *cyp1a1* (Applied Biosystems) and analyzed using a 7900 HT fast real-time polymerase chain reaction (PCR system; Applied Biosystems). Fold change values were calculated using the ΔΔCt method [32].

Statistical analysis

The mean ± standard error was determined for each treatment group. Differences between means were determined with a parametric analysis of variance. When significant differences were detected, treatment groups were compared with the appropriate control using Dunnett's two-tailed *t* test. For real-time PCR, statistical analysis was performed on the ΔCt values. Statistical analyses were performed in GraphPad Prism version 4.0a for Macintosh OS X.

RESULTS AND DISCUSSION

Intercalation of TCDD into natural K-saponite

Several recent studies have demonstrated that naturally occurring PCDDs are strongly associated with clay minerals, including both smectites and kaolinites [3–7,33]. In the case of smectites, laboratory studies have shown that dibenzo-*p*-dioxin sorption occurs in the interlamellar region of the clay [1,2]. Our objective was to prepare a clay–TCDD complex analogous to the complexes found in nature in which the sorbed TCDD is sequestered between the clay layers (i.e., is intercalated) for the studies evaluating humoral immune competence. Unlike recent in vitro studies of aryl hydrocarbon receptor-mediated activities of TCDD in mixtures with humic substances in which TCDD was simply added to dissolved humic substances [34], the objective was to determine the extent of biouptake of TCDD intercalated in saponite clay. Preparation of intercalated TCDD–clay complexes was challenging because of the exceptionally low aqueous solubility of TCDD ($<6 \times 10^{-10}$ mole/L) that precluded the use of traditional aqueous batch sorption methods to achieve this surface loading [1,2]. Based on prior TCDD-induced immune suppression studies that utilized TCDD dissolved in DMSO [35], this solvent system was used to prepare the K-saponite–TCDD complex.

DMSO is an effective solvent for solute delivery into clay interlayers, because DMSO has a high affinity for both 2:1 and 1:1 phyllosilicates [36–38]. To maximize TCDD sorption in the K-saponite interlayers while keeping the amount of TCDD sorbed on the external surface to a minimum, the minimum volume of DMSO required to expand the K-saponite clay fully was used. Overnight exposure of K-saponite to liquid DMSO resulted in a d_{001} spacing of 1.94 nm. This d_{001} spacing corresponds to an intercalation of two layers of DMSO in the K-saponite based on an approximate molecular thickness of DMSO of 0.47 nm based on its molecular structure.

A two-layer expansion of K-saponite by the DMSO–TCDD solution was achieved by adding the minimum volume of DMSO that would expand the interlayer by 1.0 nm. The resulting d_{001} spacing of this complex was 1.92 nm, as shown in Figure 1. The TGA mass loss curve of the expanded K-saponite–DMSO–TCDD complex is shown in Figure 2 (top). Of the 33.3% of mass added by the DMSO, 30.8% was removed after isothermal heating of the clay at 200°C for 50 min (bottom of Fig. 2) and 34.9% total mass was lost after heating to 1,000°C (top of Fig. 2). Given that the melting and boiling points of TCDD (305 and 447°C, respectively) are much greater than those of DMSO (19 and 189°C, respectively), it was assumed that little, if any, of the TCDD was removed by the isothermal heating of the clay at

200°C for 50 min [39]. The d_{001} spacing of the K-saponite–DMSO–TCDD complex was 1.35 nm after the 200°C isothermal treatment (Fig. 1).

The target concentration of 50 mg TCDD/kg clay corresponds to a surface loading of 0.005% TCDD, or 155 nmoles TCDD/g clay. The XRD and TGA data provide essential baseline characterization data for these complexes, but these methods lack the sensitivity to detect the intercalated TCDD directly at this low surface coverage. The FTIR spectroscopy was used to detect the presence of TCDD sorbed to K-saponite (after intercalation with DMSO). To the best of our knowledge, Raman or FTIR spectra of TCDD in the solid phase have not previously been reported. Vapor-phase spectra of TCDD and other chlorinated congeners have been reported [40,41]. Using the drop-coating deposition method, μ-Raman and μ-FTIR spectra of solid phase TCDD crystals were obtained (Fig. 3, spectra B and C, respectively). For comparison, theoretical infrared and Raman spectra were calculated using density functional theory, and these results are included in Figure 3 (spectra A and C). As shown, good agreement between the experimental and predicted spectra was observed.

The FTIR spectrum of sorbed TCDD on the natural K-saponite sample at a surface loading of 50 mg TCDD/kg clay is shown in Figure 3 (spectrum E). This spectrum was obtained by spectral subtraction of the diffuse reflectance FTIR spectrum of K-saponite–DMSO from that of the K-saponite–DMSO–TCDD complex. Residual DMSO retained by these clay–organic complexes resulted in some spectral interference. However, the resulting difference spectrum contains the main spectral features of TCDD.

Synthetic saponite

Structural, thermal, and spectroscopic characterization data of the natural SapCa-2 saponite clay have been reported previously [2,42]. Whereas natural saponite has a regularly stacked layered structure with a basal spacing of approximately 1.2 nm, synthetic saponite has a delaminated structure in which the 0.96-μm-thick nanolayers are irregularly aggregated into disordered bundles. As shown by the powder diffraction pattern in Figure 4, the absence of a 001 diffraction peak verifies a delaminated structure. All of the observed peaks in the pattern are in-plane <hk0> reflections of the atomically ordered layers. The transmission electron microscope image shown in Figure 5 confirms the disordered aggregation of nano-layers. Evident in the micrograph are disordered aggregates of individual nanolayers approximately 10 to 50 nm in diameter. There is no evidence for the regular stacking of layers. The ^{29}Si MAS NMR spectrum of synthetic saponite exhibits the presence of two resonances, as expected for a 2:1 clay layer structure in which the negative charge on the layer arises from the partial replacement of silicon by aluminum [28]. A −85.4 ppm resonance is assigned to Si centers linked through bridging oxygen atoms to three tetrahedral Si ions and one tetrahedral Al ion (i.e., Q^3 sites), and a −92.7 ppm resonance is ascribed to Si linked through bridging oxygen to four Si neighbors (i.e., Q^4 sites). The ^{27}Al MAS NMR spectrum of saponite contains two signals at chemical shifts of 61.6 ppm and 10.5 ppm, which is in agreement with the presence of Al in both the tetrahedral and the octahedral positions, respectively, of a 2:1 layered silicate structure. These latter results are in agreement with the spectra previously reported for delaminated saponite clay [28]. The delaminated synthetic saponite provides a different physical arrangement of clay layers compared with the natural

saponite that forms a regularly stacked layered structure. In the synthetic saponite, TCDD was uniformly distributed on the basal surfaces of clay monolayers comprising the disordered aggregates, possibly manifesting greater accessibility compared with TCDD intercalated between the regularly stacked clay layers in natural saponite.

TCDD adsorbed on clay suppressed humoral immune function

With the demonstration that TCDD could be adsorbed on either synthetic saponite or natural K-saponite, the effects of the vehicle on TCDD-induced suppression of immune function were determined, which is well characterized as a sensitive target of toxicity by TCDD [43]. Prior to assessment of immune function, the biodistribution of TCDD delivered in corn oil or adsorbed on saponites was verified using induction of *cyp1a1* gene expression in the liver. As can be seen in Figure 6, *cyp1a1* gene expression was robustly induced in the liver regardless of the vehicle used to deliver the TCDD. These results demonstrate absorption from the gastrointestinal tract following TCDD administration by oral gavage. Next, immune function was evaluated by determining the effect of TCDD administration on elicitation of antigen-specific (sheep erythrocytes) IgM AFCs. The TCDD suppressed the sRBC-induced AFC response, in a dose-responsive manner, regardless of the vehicle used to deliver the TCDD (Fig. 7). Collectively, these results demonstrate that TCDD adsorbed on saponites is absorbed from the GI tract and suppresses immune function following oral administration.

In vivo, TCDD induced *cyp1a1* gene expression in the liver and suppressed humoral immunity regardless of whether TCDD was delivered in corn oil or adsorbed on synthetic or natural K-saponite. With the TCDD-adsorbed natural K-saponite as a model for one component of contaminated soil, these results suggest that TCDD is absorbed from the GI tract and compromises immune function following oral exposure. The present study also confirms our previous finding that TCDD adsorbed on amorphous silica also suppressed immune function [35]. Currently, it is unknown how TCDD is distributed from the GI tract when adsorbed onto the saponites. Possibilities include displacement from the saponite or, less likely, dissolution of the saponite, allowing free TCDD to be absorbed in the GI tract. It is also plausible that the TCDD-adsorbed saponite is engulfed by various antigen-presenting cells, such as Kuppfer cells in the liver, which likely contributes to the *cyp1a1* induction, and dendritic cells in the spleen, to further contribute to the immune suppression [35]. Additional studies are needed to discern the mechanisms by which TCDD is absorbed following oral administration when adsorbed on saponites.

CONCLUSION

The long-term goal of this research is to contribute to a better understanding of bioavailability processes involving TCDD-contaminated soils and sediments. Because these materials are diverse, complex, and heterogeneous, we seek to evaluate bioavailability processes involving individual geosorbent types that plausibly function as sorbents for TCDD in natural environments. The present study compared the suppression of humoral immune responses by TCDD dissolved in corn oil with that by TCDD intercalated in a smectite clay (saponite); this type of experiment measures the relative bioavailability of

TCDD [18]. Because the existing data on the oral bioavailabilities of soiland sediment-bound TCDD are in conflict [19], regulatory agencies often adopt a conservative approach in risk assessment by assuming that the total contaminant present in soil or sediment is available for uptake by possible receptors [18]. Others contend that the soil- or sediment-bound contaminants, including PCDD/Fs, are unavailable for uptake [44]; accordingly, it is argued that the default assumption of 100% bioavailability of PCDD/Fs leads to unnecessarily stringent regulatory criteria [21,22], and remediation endpoints should be evaluated on the basis of freely dissolved concentrations rather than total concentrations, especially when contaminants are adsorbed primarily by carbonaceous geosorbents [17,45]. However, because sorption of TCDD and other sparingly soluble NOCs often results from a combination of partitioning into amorphous organic matter, adsorption of carbonaceous geosorbents, and intercalation by clays, the aggregate bioavailability plausibly depends on the distribution of the sorbed contaminant among these geosorbents, assuming that each manifests differential effects on bioavailability processes. The similar relative bioavailability of TCDD delivered in CO or adsorbed on natural or synthetic saponite in the present study, or adsorbed on silica in a previous study [35], is consistent with previous reports of TCDD biouptake from ball clays by livestock [26,27] and humans [24]. These results are in contrast to the substantial reductions in biouptake (for example, by aquatic worms or clams) of several poorly water-soluble NOCs sorbed predominately by carbonaceous geosorbents [17], suggesting sorbent-specific effects on bioavailability processes pertaining to TCDD. In this context, TCDD adsorbed by clays is likely to be highly available for biouptake and biodistribution in mammals, and this should be considered in risk assessment and the development of remediation goals, especially for sites where clays represent a significant sorptive sink for TCDD.

Acknowledgments

This project received financial support from grant P42 ES004911 from the National Institute of Environmental Health Science, National Institute of Health; from grant 2008-35107-04548 from the U.S. Department of Agriculture; and from the Michigan Agricultural Experimental Station.

References

1. Liu C, Li H, Teppen BJ, Johnston CT, Boyd SA. Mechanisms associated with the high adsorption of dibenzo-*p*-dioxin from water by smectite clays. Environ Sci Technol. 2009; 43:2777–2783. [PubMed: 19475949]
2. Rana K, Boyd SA, Teppen BJ, Li H, Liu C. Probing the microscopic hydrophobicity of smectite surfaces: A vibrational spectroscopic study of dibenzo-*p*-dioxin sorption to smectite. Physical Chem Chem Physics. 2009; 11:2976–2985.
3. Ferrario J, Byrne C. Dibenzo-*p*-dioxins in the environment from ceramics and pottery produced from ball clay mined in the United States. Chemosphere. 2002; 46:1297–1301. [PubMed: 12002454]
4. Ferrario J, Byrne C, Schaum J. Concentrations of polychlorinated dibenzo-*p*-dioxins in processed ball clay from the United States. Chemosphere. 2007; 67:1816–1821. [PubMed: 17223172]
5. Ferrario J, Byrne CJ, Cleverly DH. 2,3,7,8-Dibenzo-*p*-dioxins in mined clay products from the United States: Evidence for possible natural origin. Environ Sci Technol. 2000; 34:4524–4532.
6. Gadomski D, Tysklind M, Irvine RL, Burns PC, Andersson R. Investigations into the vertical distribution of PCDDs and mineralogy in three ball clay cores from the United States exhibiting the natural formation pattern. Environ Sci Technol. 2004; 38:4956–4963. [PubMed: 15506186]

7. Schmitz M, Scheeder G, Bernau S, Dohrmann R, Germann K. Dioxins in primary kaolin and secondary kaolinitic clays. Environ Sci Technol. 2010; 45:461–467. [PubMed: 21126071]
8. Gaus C, Brunskill GJ, Connell DW, Prange J, Muller JF, Papke O, Weber R. Transformation processes, pathways, and possible sources of distinctive polychlorinated dibenzo-*p*-dioxin signatures in sink environments. Environ Sci Technol. 2002; 36:3542–3549. [PubMed: 12214647]
9. Prange JA, Gaus C, Papke O, Muller JF. Investigations into the PCDD contamination of topsoil, river sediments and kaolinite clay in Queensland, Australia. Chemophere. 2002; 46:1335–1342.
10. Boyd, SA., Johnston, CT., Laird, DA., Teppen, BJ., Li, H. Comprehensive study of organic contaminant adsorption by clays: Methodologies and mechanisms. In: Xing, B.Senesi, N., Huang, PM., editors. Biophysico-Chemical Processes of Anthropogenic Organic Compounds in Environmental Systems. John Wiley&Sons; New York, NY, USA: 2011. p. 51-71.
11. Boyd SA, Sheng G, Teppen BJ, Johnston CT. Mechanisms for the adsorption of substituted nitrobenzenes by smectite clays. Environ Sci Technol. 2001; 35:4227–4234. [PubMed: 11718335]
12. Sheng G, Johnston CT, Teppen BJ, Boyd SA. Adsorption of dinitrophenol herbicides from water by montmorillonites. Clays Clay Miner. 2002; 50:25–34.
13. Li H, Teppen BJ, Johnston CT, Boyd SA. Thermodynamics of nitroaromatic compound adsorption from water by smectite clay. Environ Sci Technol. 2004; 38:5433–5442. [PubMed: 15543748]
14. Johnston CT, De Oliveira MF, Teppen BJ, Sheng G, Boyd SA. Spectroscopic study of nitroaromatic-smectite sorption mechanisms. Environ Sci Technol. 2001; 35:4767–4772. [PubMed: 11775151]
15. Chiou CT, Kile DE. Deviations from sorption linearity on soils of polar and nonpolar organic compounds at low relative concentrations. Environ Sci Technol. 1998; 32:338–343.
16. Chiou CT, Kile DE, Rutherford DW, Sheng G, Boyd SA. Sorption of selected organic compounds from water to a peat soil and its humic-acid and humin fractions: Potential sources of the sorption nonlinearity. Environ Sci Technol. 2000; 34:1254–1258.
17. Cornelissen G, Gustafsson O, Bucheli TD, Jonker MTO, Koelmans AA, van Noort PCM. Extensive sorption of organic compounds to black carbon, coal, and kerogen in sediments and soils: Mechanisms and consequences for distribution, bioaccumulation, and biodegradation. Environ Sci Technol. 2005; 39:6881–6895. [PubMed: 16201609]
18. National Research Council. Bioavailability of Contaminants in Soils and Sediments. National Academies; Washington, DC: 2003.
19. Kimbrough RD, Krouskas CA, Carson ML, Long TF, Bevan C, Tardiff RG. Human uptake of persistent chemicals from contaminated soil: PCDD/Fs and PCBs. Regul Toxicol Pharmacol. 2010; 57:43–54. [PubMed: 20035816]
20. Zwiernik MJ, Quensen JF, Boyd SA. Residual petroleum in sediments reduces the bioavailability and rate of reductive dechlorination of aroclor 1242. Environ Sci Technol. 1999; 33:3574–3578.
21. Chai Y, Davis JD, Wilken M, Artin GD, Mowery DM, Gosh U. Role of black carbon in the distribution of polychlorinated dibenzo-*p*-dioxins/dibenzofurans in aged field contaminated soils. Chemophere. 2011; 82:639–647.
22. Budinsky RA, Rowlands JC, Casteel S, Pent G, Cushing GA, Newsted I, Giesy JP, Ruby MV, Alward LL. A pilot study of oral bioavailability of dioxins and furans from contaminated soils: Impact of differential hepatic enzyme activity and species differences. Chemophere. 2008; 70:1774–1786.
23. Rudy MV, Fehling KA, Paustenbach DJ, Landenberger DJ, Holsapple MP. Oral bioaccessibility of dioxins/furans at low concentrations (50–350 ppt toxicity equivalent) in soil. Environ Sci Technol. 2002; 36:4905–4911. [PubMed: 12487316]
24. Franzblau A, Hedgeman E, Chen Q, Lee SY, Adriaens P, Bemond A, Garabrant D, Gillespie BW, Hong B, Jolliet O, Lepkowski J, Lukesemburg W, Maier M, Wenger Y. Human exposure to dioxins from clay: A case report. Environ Health Perspect. 2008; 116:238–242. [PubMed: 18288324]
25. Ferrario J, Byrne C, Lorber M, Saunders P, Williams LB, Dupuy AE, Winters D, Cleverly DH, Schaum J, Pinsky P, Deyup C, Ellis R, Walcot J. A statistical survey of dioxin-like compounds in United States poultry. Organohalogen Compounds. 1997; 34:245–251.

26. Hayward DG, Bolger PM. Tetrachlorodibenzo-*p*-dioxin in baby food made from chicken produced before and after the termination of ball clay use in chicken feed in the United States. Environ Res. 2005; 99:307–313. [PubMed: 16307972]
27. Hayward DG, Nortrup D, Gardner A, Clower M. Elevated TCDD in chicken eggs and farm-raised catfish fed a diet with ball clay from a southern United States mine. Environ Res. 1999; 81:248–256. [PubMed: 10585021]
28. Shao H, Pinnavaia TJ. Synthesis and properties of nanoparticle forms saponite clay, cancrinite zeolite and phase mixtures thereof. Microporous Mesoporous Mater. 2010; 133:10–17. [PubMed: 21709774]
29. Vogels RJMJ, Kerkhoffs MJHV, Geus JW. Preparation of catalysts VI—Scientific bases for the preparation of heterogeneous catalysts. Stud Surf Sci Catal. 1995; 91:1153–1161.
30. Zhang DM, Xie Y, Mrozek MF, Ortiz C, Davisson VJ, Ben-Amotz D. Raman detection of proteomic analytes. Anal Chem. 2003; 75:5703–5709. [PubMed: 14588009]
31. Jerne NK, Nordin AA. Plaque formation in agar by single antibody-producing cells. Science. 1963; 140:405.
32. Livak KJ, Schmittgen TD. Analysis of relative gene expression data using real-time quantitative PCR and the 2–Delta Delta Ct method. Methods. 2001; 25:402–408. [PubMed: 11846609]
33. Gaus C, Brunskill GJ, Weber R, Papke O, Muller JF. Historical PCDD inputs and their source implications from dated sediment cores in Queensland (Australia). Environ Sci Technol. 2001; 35:4597–4603. [PubMed: 11770761]
34. Bittner M, Hilscherova K, Giesy JP. In vitro assessment of AhR-mediated activities of TCDD in mixture with humic substances. Chemosphere. 2009; 76:1505–1508. [PubMed: 19616275]
35. Kaplan BL, Crawford RB, Kovalova N, Arencibia A, Kim SS, Pinnavaia TJ, Boyd SA, Teppen BJ, Kaminski NE. TCDD adsorbed on silica as a model for TCDD contaminated soils: Evidence for suppression of humoral immunity in mice. Toxicology. 2011; 282:82–87. [PubMed: 21272611]
36. Dios-Cancela G, Alfonso-Mendez L, Huertas FJ, Romero-Taboada E, Sainz-Diaz CI, Hernandez-Laguna A. Adsorption mechanism and structure of the montmorillonite complexes with (CH_3)(2)XO (X=C, and S), (CH_3O)(3)PO, and CH_3-CN molecules. J Colloid Interf Sci. 2000; 222:125–136.
37. Letaief S, Tonle IK, Diaco T, Detellier C. Nanohybrid materials from interlayer functionalization of kaolinite: Application to the electrochemical preconcentration of cyanide. Appl Clay Sci. 2008; 42:95–101.
38. Johnston CT, Sposito G, Bpcian DF, Birge RR. Vibrational spectroscopic study of the interlamellar kaolinite-dimethylsulfoxide complex. J Phys Chem. 1984; 88:5959–5964.
39. Shiu WY, Ma KC. Temperature dependence of physical—Chemical properties of selected chemicals of environmental interest. II. Chlorobenzenes, polychlorinated biphenyls, polychlorinated dibenzo-*p*-dioxins, and dibenzofurans. J Phys Chem Ref Data. 2000; 29:387–462.
40. Grainger J, Gelbaum LT. Tetrachlorodibenzo-*para*-dioxin isomer differentiation by capillary gas chromatography Fourier transform–infrared spectroscopy. Appl Spectrosc. 1987; 41:809–820.
41. Grainger J, Reddy VV, Patterson PG. Molecular-geometry approximations for chlorinated dibenzodioxins by Fourier-transform infrared spectroscopy. Appl Spectrosc. 1988; 42:643–655.
42. Ras RHA, Johnston CT, Franses EI, Ramaekers R, Maes G, Foubert P, DeSchryver FC, Schoonheydt RA. Polarized infrared study of hybrid Langmuir–Blodgett monolayers containing clay mineral nanoparticles. Langmuir. 2003; 19:4295–4302.
43. Sulentic CE, Kaminski NE. The long winding road toward understanding the molecular mechanisms for B-cell suppression by 2,3,7,8-tetrachlorodibenzo-*p*-dioxin. Toxicol Sci. 2011; 120(Suppl):171–191.
44. Alexander M. Aging, bioavailability, and overestimation of risk from environmental pollutants. Environ Sci Technol. 2000; 34:4259–4265.
45. Ghosh U, Luthy RG, Cornelissen G, Werner D, Menzie CA. In-situ sorbent amendments: A new direction in contaminated sediment management. Environ Sci Technol. 2011; 45:1163–1168. [PubMed: 21247210]

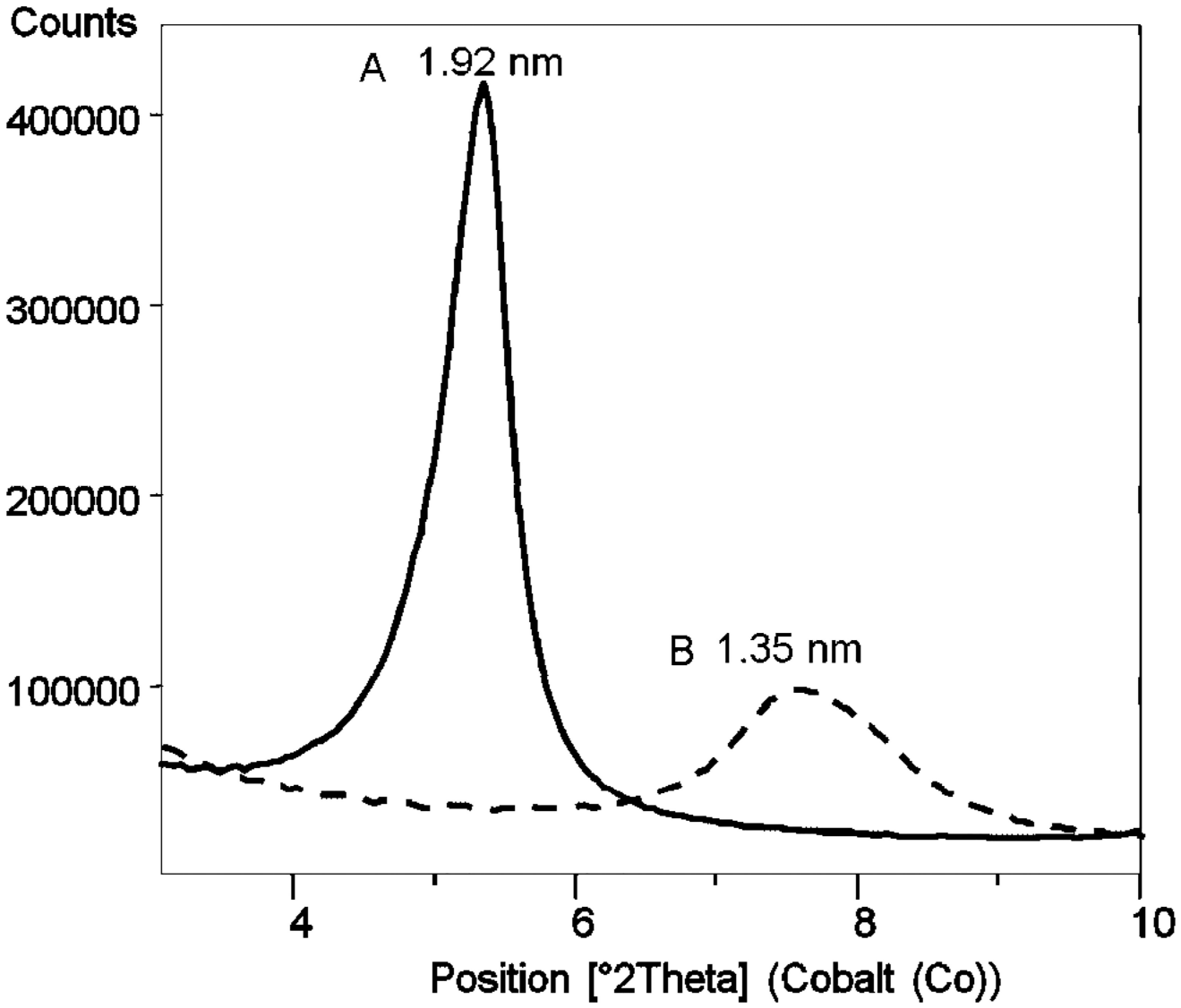

Fig. 1.

X-ray powder diffraction pattern of natural K-saponite clay treated with dimethylsulfoxide and dioxin heated at 60°C (A) and after isothermal heat treatment at 200°C (B).

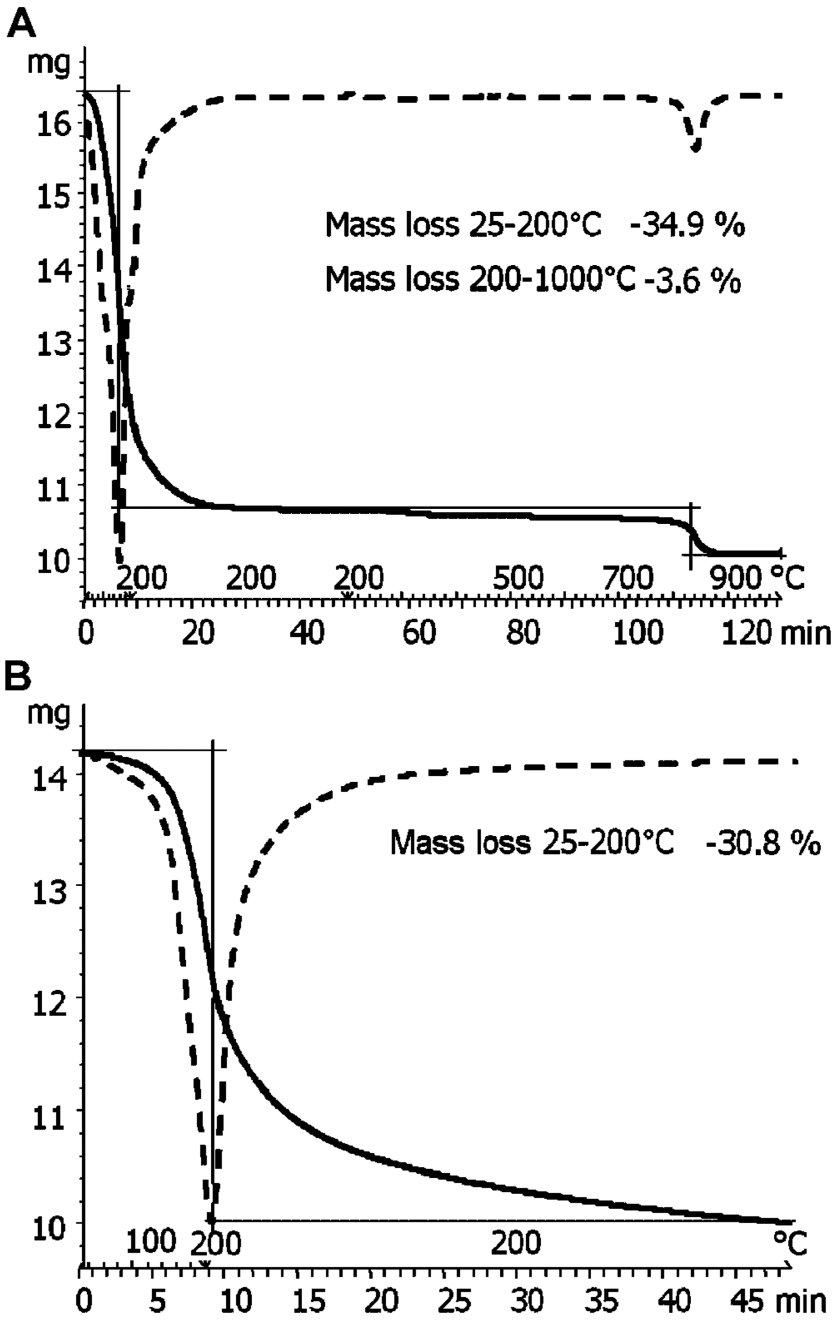

Fig. 2.

Thermogravimetric analysis (TGA) of tetrachlorodibenzo-*p*-dioxin–dimethylsulfoxide (DMSO)–K-saponite mixture heated at 60°C or heated at 1,000°C (**A**) and undergoing isothermal heat treatment at 200°C (**B**). The solid curve indicates DMSO mass loss; the dashed line curve is the TGA curves of the first derivative.

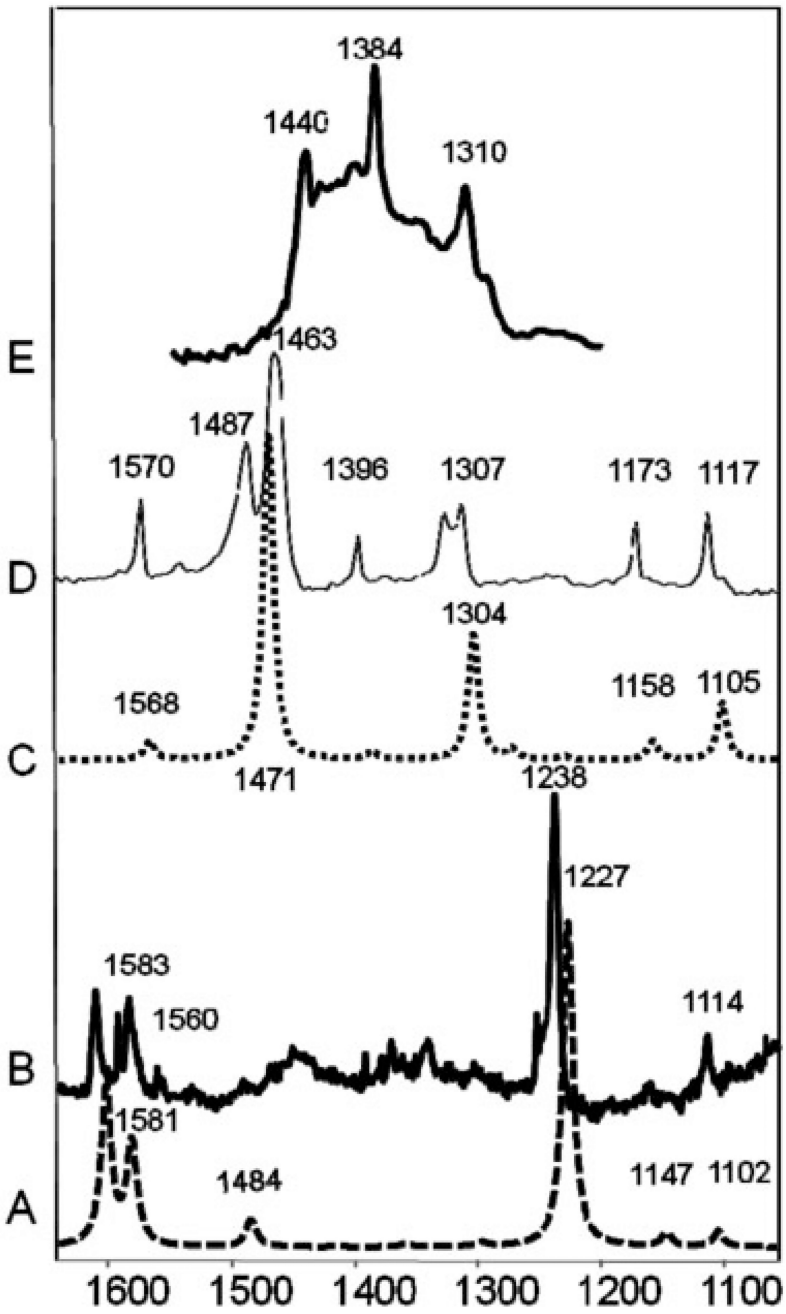

Fig. 3.

Comparison of Fourier transform infrared (FTIR) and Raman spectra of tetrachlorodibenzo-*p*-dioxin (TCDD). A: Theoretical Raman spectra. B: Measured Raman crystal TCDD spectra. C: Theoretical FTIR TCDD spectra. D: Measured micro-FTIR crystal TCDD spectra. E: Measured FTIR spectra of TCDD adsorbed to K-saponite clay.

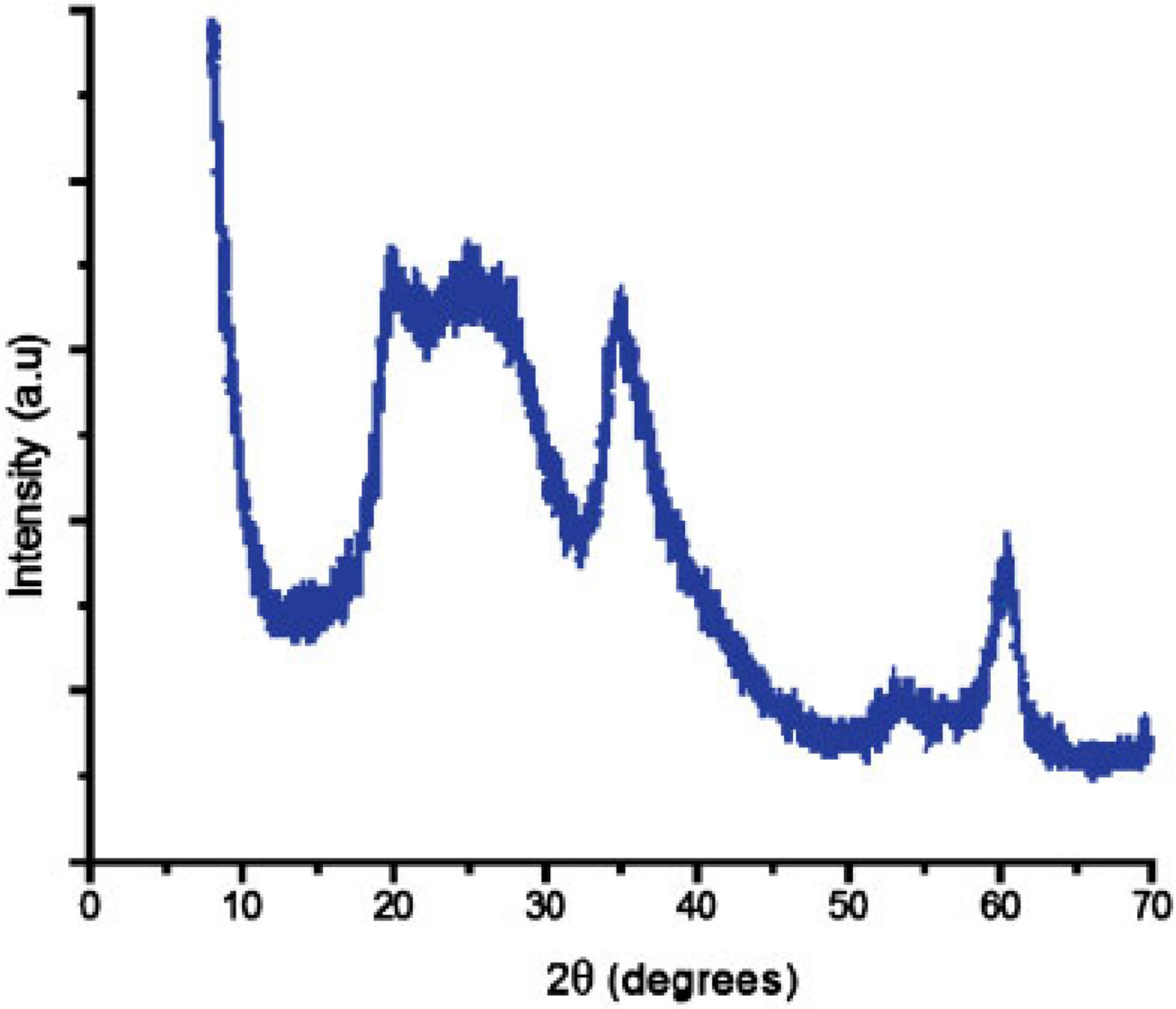

Fig. 4.
X-ray powder diffraction pattern of synthetic saponite. a.u.= Arbitrary units.

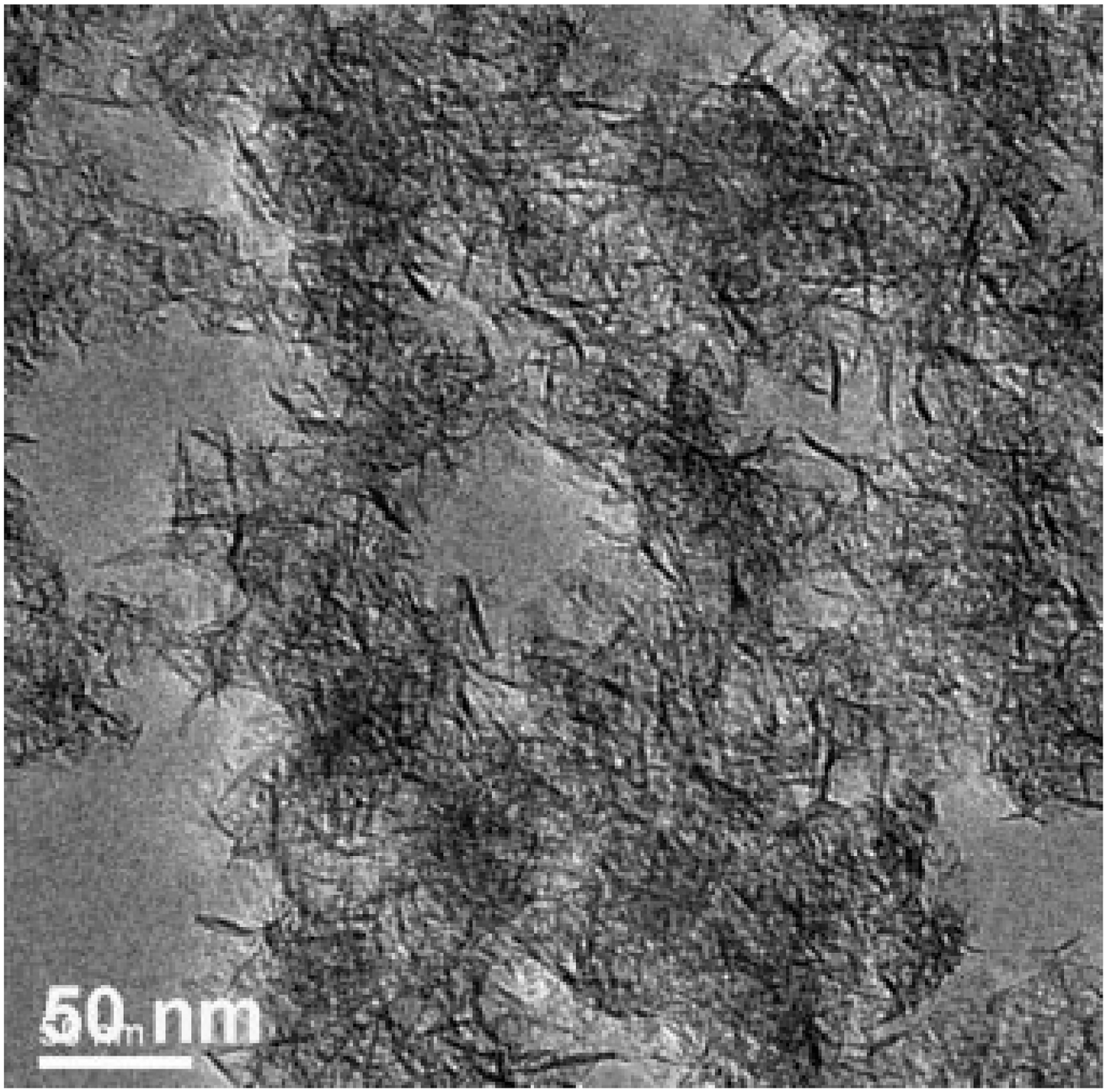

Fig. 5.
Transmission electron microscopy image of synthetic saponite formed at 90°C.

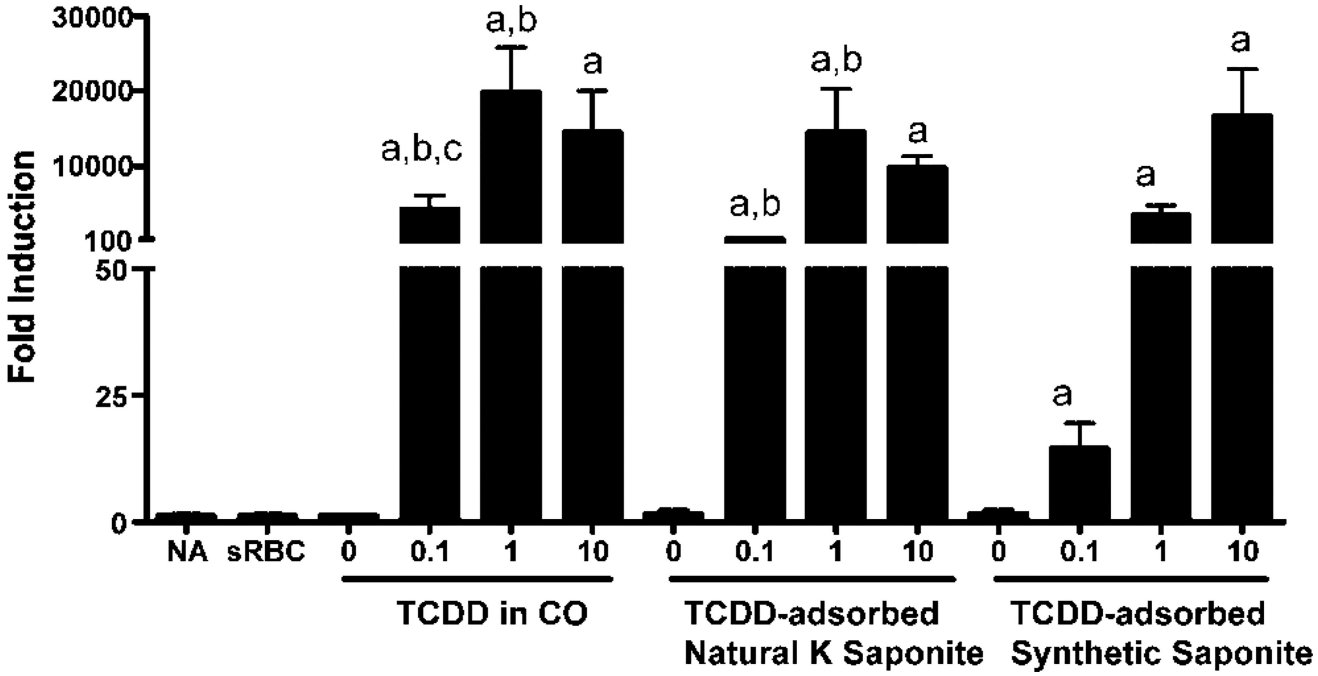

Fig. 6.

Tetrachlorodibenzo-*p*-dioxin (TCDD)-induced *cyp1a1* gene expression in liver. Mice were treated with TCDD in corn oil (CO) or TCDD-adsorbed synthetic or natural K-saponite (0–10 μg/kg/d) for 4 d by oral gavage. 0 in each group indicates CO, natural or synthetic K-saponite without TCDD. On day 3, mice were sensitized with sRBC. Expression of *cyp1a1* gene was evaluated 4 d after sRBC by real-time PCR. $^{a}p < 0.05$ as compared with vehicle (0); $^{b}p < 0.05$ as compared with TCDD-adsorbed synthetic saponite; $^{c}p < 0.05$ as compared with TCDD-adsorbed natural K-saponite.

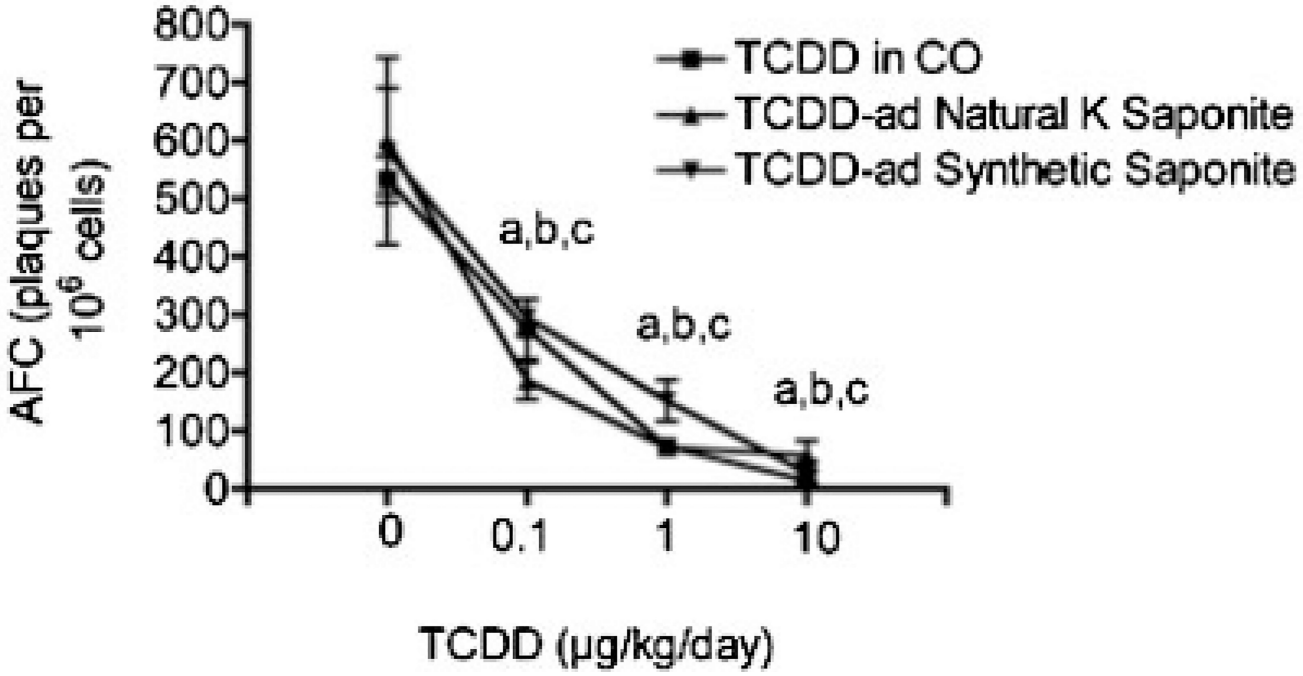

Fig. 7.

Tetrachlorodibenzo-*p*-dioxin (TCDD)-induced suppression of humoral immunity. Mice were treated as described in Fig. 6. The number of IgM-producing cells (AFC) was quantified 4 d after sRBC by plaque assay. $^{a–c}p < 0.05$ as compared with vehicles (0) for TCDD in CO, TCDD-adsorbed natural K-saponite and TCDD, and TCDD-adsorbed synthetic saponite, respectively.